Structural Analysis of Collapsed, and Twisted and Collapsed, Multiwalled Carbon Nanotubes by Atomic Force Microscopy

Min-Feng Yu,[1] Tomasz Kowalewski,[2,*] and Rodney S. Ruoff[1,†]

[1]*Department of Physics, Washington University in St. Louis, St. Louis, Missouri 63130*
[2]*Department of Chemistry, Washington University in St. Louis, St. Louis, Missouri 63130*

(Received 16 May 2000)

A fully collapsed multiwalled carbon nanotube (MWCNT1) section and a different twisted and fully collapsed MWCNT were observed with tapping-mode atomic force microscopy. The collapsed section of MWCNT1 was significantly more flexible than the uncollapsed sections, and advanced 120 nm within 1 month. The collapse of MWCNT1 was most likely initiated by its interaction with the surface, and possibly a water meniscus. The ability of carbon nanotubes to radially deform under the influence of surface interactions is in striking contrast with their extremely high axial rigidity.

DOI: 10.1103/PhysRevLett.86.87 PACS numbers: 61.48.+c, 61.16.Ch, 62.20.Fe

Carbon nanotubes (NTs) have been predicted to have high modulus and strength [1–3], and experiments confirm this [4–9]. NTs appear to be excellent candidates for reinforcement in composites. The high in-plane rigidity of graphene sheets contrasts with their out-of-plane flexibility, which is responsible for the considerable radial deformability of carbon NTs [10]. NTs in various states of radial deformation, including the collapsed (ribbonlike) state, have been observed in transmission electron microscopy (TEM) [11–14]. The radial deformability of NTs has been recently studied quantitatively with the aid of atomic force microscopy (AFM) [15–17], and radial deformation has also been found to prominently affect NT electrical properties [18,19]. The susceptibility of NTs to collapse should be relevant to their future applications as components in molecular devices.

We present the results of AFM observations of multiwalled carbon nanotubes (MWCNTs), which clearly show that radial deformation and collapse can be induced, and stabilized, by substrate-nanotube interactions.

The MWCNTs used in the experiments were synthesized by the arc method, purified by oxidation in air, and had diameters ranging from 2–50 nm [20].

Figure 1 shows a 2.8-μm-long MWCNT (MWCNT1) with a ~800-nm-long interior section (between the two arrows) of distinctly different appearance. Both the height image [Fig. 1(a)] and the corresponding amplitude image [Fig. 1(b)] show that this section of MWCNT1 has a flat ribbonlike shape—it is collapsed. (Additional AFM images showed that most MWCNTs crossing the substrate trenches were essentially straight, which emphasizes their mechanical stiffness.) A height profile [Fig. 1(c)] along MWCNT1 [between points 1 and 2 as marked in Fig. 1(a)] shows that the collapsed section drops by ~8 nm over the trench. Figure 2(b) shows a typical height profile across the collapsed section; it has an average height of ~2.3 nm and a "pillow" shape. In contrast, the height of the uncollapsed section of MWCNT1 [section profile, Fig. 2(a)] is equal to ~6.5 nm.

The shape of MWCNT1 can be reconstructed from the AFM image as follows [21]. The profile of the tip in the direction perpendicular to the long axis of MWCNT1 was obtained by eroding the profile of the uncollapsed section shown in Fig. 2(a) with the expected profile of MWCNT1. Subsequently, the obtained tip profile was eroded from the profile of the collapsed section, and the height of uncertain parts of the reconstructed profile was set to zero [Fig. 2(b)]. The tip reconstruction was performed with a range of elliptical shapes for the profile of MWCNT1 while seeking consistency between the perimeter length of the reconstructed profile of the collapsed section, P_{rc}, and the perimeter length of the uncollapsed section, P_{ru}, for the assumed shape (see Ref. [22] for further details). It is clear that even the "uncollapsed" section is significantly flattened; since the perimeter consistency ($P_{rc}/P_{ru} \approx 1$)

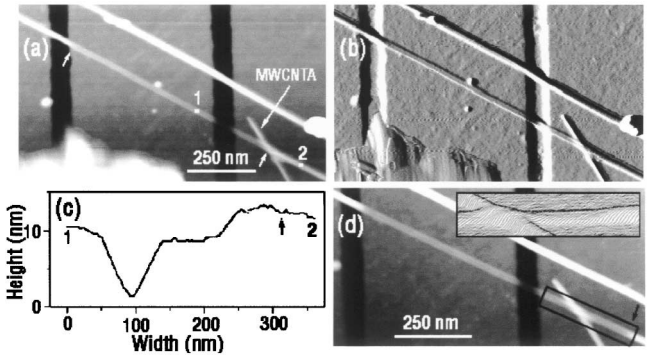

FIG. 1. Collapse of a MWCNT (MWCNT1) deposited on a patterned silicon wafer as visualized with tapping-mode AFM. The height in this and all subsequent images was coded in grayscale, with darker tones corresponding to lower features. An 800-nm-long collapsed section is evident in MWCNT1 as marked by the arrows. Two-dimensional height (a) and amplitude (b) images of the same area are shown. (c) Height profile taken between point 1 and 2 along MWCNT1 marked in (a). (d) MWCNT1 was reimaged after a period of one month storage at ambient conditions. Notice that the collapse propagated another ~120 nm (indicated with an arrow). The inset in (d) shows the surface plot of the enclosed square region in (d).

 © 2000 The American Physical Society

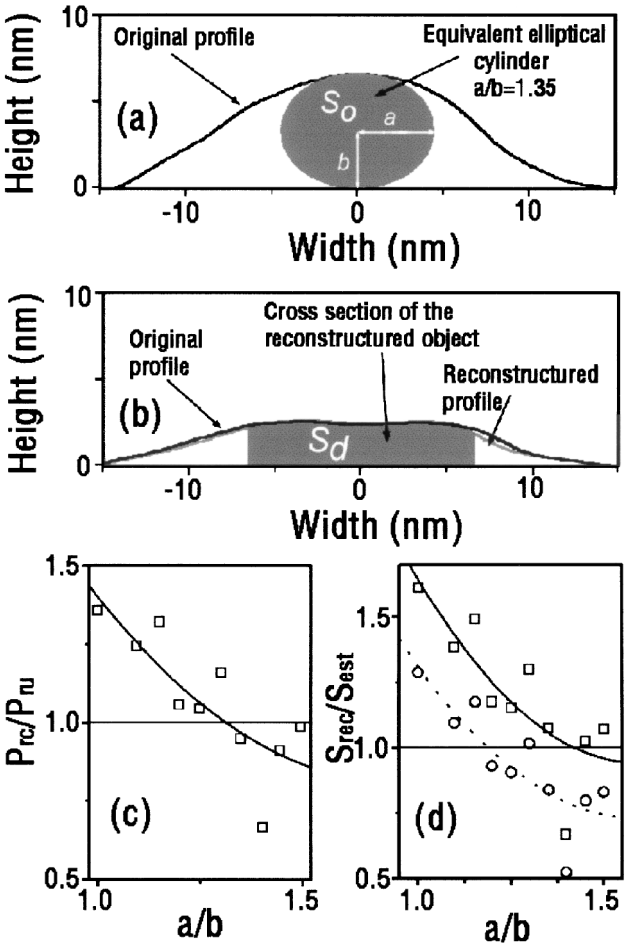

FIG. 2. Reconstruction of MWCNT1 from the AFM images. (a) Height profile taken across uncollapsed MWCNT1 in (a) and the obtained elliptical cross section of MWCNT1 following the reconstruction procedure explained in the text. (b) Height profile taken across collapsed MWCNT1 in (a), and the reconstructed height profile and approximate cross section of the collapsed MWCNT1 following the reconstruction procedure explained in the text. (c) Perimeter fit for nanotube ellipses having different axis ratio a/b. (d) Area fits for three layer (□) and four layer (○) nanotube ellipses having different axis ratio a/b.

was achieved for $a/b = 1.35$ [Fig. 2(c)], where a/b denotes the ratio between the horizontal and vertical axes of the ellipse.

The cross-section areas of reconstructed profiles of the collapsed section, S_{rec}, were compared with the geometrically calculated values. The cross-section area of a fully collapsed MWCNT1 can be calculated as $S_{\text{est}} = \pi R_{\text{ext}}^2 - \pi(R_{\text{ext}} - nd)^2$, where $R_{\text{ext}} = (ab)^{1/2}$ denotes the external radius of the uncollapsed section in its undeformed (cylindrical) shape, n is the number of walls, and $d = 0.34$ nm is the interlayer spacing. Figure 2(d) shows the results in the form of plots of $S_{\text{rec}}/S_{\text{est}}$ vs a/b, for values of $n = 3$ and $n = 4$. For $n = 4$, consistency between cross sections is achieved for $a/b \approx 1.2$, whereas for $n = 3$, $a/b \approx 1.35$. Since only the latter value agrees with the perimeter analysis, MWCNT1 is determined to be a 3-cylinder MWNT, consistent with the height of the collapsed section (2.3 nm) being close to the thickness of six graphene sheets (thickness 0.34 nm). In a perfectly cylindrical state, the inner diameter of this 3-walled NT would be 5.5 nm.

For a given number of walls, full collapse of a MWCNT can occur only above some critical radius of the innermost tube. According to simulations based on TEM analysis of a collapsed MWCNT, the critical radius for a stable 3-cylinder MWCNT is between 4 nm and 7 nm [23].

The transition from the partially flattened to collapsed state requires external energy to overcome the barrier separating these two states. One of the pathways along which the necessary energy can be supplied may involve bending of the NT beyond the point of buckling. In the case of MWCNT1 this event might have been triggered upon adsorption on the surface, when MWCNT1 crossed MWCNTA [Fig. 1(b)]. Subsequently, the collapse extended up to the second trench on the left [Fig. 1(b)], where it was arrested due to the sudden decrease of the attractive substrate force (the trench is 17 nm deep). Because of this energy barrier, the physical boundary between these states ought to be metastable, and the collapsed state might advance. Such was indeed observed in the case of MWCNT1, when it was imaged one month later. As shown in Fig. 1(d), the zone of collapse advanced to the right by ~120 nm (see arrow).

The importance of surface-NT interactions in maintaining the collapsed state of MWCNT1 was assessed by calculating the energy balance between the mechanical deformation and surface interactions. The total increase of strain energy upon flattening (per unit length per NT layer) was calculated as $\Delta E_s = E_b - E_{nt}$, where $E_{nt} = \pi k/R$ denotes the strain energy of a cylindrical shell of radius R and curvature modulus k [13], and $E_b = \pi k/r_i$ is the strain energy of high-curvature bulbs at the edges of a collapsed NT. The bulbs were each assumed to have a semicircular shape with the radius $r_i = [(2i - 1)d]/2$, where i is the shell number (counting from the inside) and $d = 0.34$ nm is the interlayer distance in the NT. The total decrease of the surface free energy (per unit length), due to the closure of the hollow core and due to the increase of the contact area with the substrate, was calculated as $\Delta E_\nu = E_{n\nu} + E_{sn\nu}$, where $E_{n\nu} = -2\gamma_n L$ and $E_{sn\nu} = -W_{sn} L$, γ_n is the surface free energy of graphite, W_{sn} is the work of adhesion between silicon and graphite surfaces, and L is the contact width and is equal to $\pi(R_{\text{int}} + d/2 - r_1)$ ($R_{\text{int}} = 2.75$ nm is the internal radius of undeformed MWCNT1). Collapse is favored if the overall energy change $\Delta E_s + \Delta E_\nu < 0$. For MWCNT1, which has three layers, an inner diameter of 5.5 nm, and an outer diameter of 7.5 nm, the results are $\Delta E_s = 36$ eV/nm and $\Delta E_\nu = -18$ eV/nm + $E_{sn\nu}$. In the calculation, $k = 1.4$ eV [13] and $\gamma_n = 1.05$ eV/nm^2 [24]. These estimates indicate that the stability of the collapsed state of MWCNT1 requires the contribution due to adhesion between MWCNT1 and the substrate to

satisfy the condition $E_{sn\nu} \leq -18$ eV/nm. Based on this condition, the work of adhesion between MWCNT1 and substrate has to be greater or equal to 2.1 eV/nm^2 (or 330 mJ/m^2). This condition is essentially satisfied here, since the typical surface energy value for silicon dioxide, γ_{SiO_2}, is in the range of 115–200 mJ/m^2 [25] and for graphite, γ_g, is reported as 165–200 mJ/m^2 [24]. Note that the surface energy of bare silicon is much higher (1400 mJ/m^2, Ref. [26]), but we used a silicon substrate with a thick oxide layer. Using 165 mJ/m^2 for the surface energy of graphite and, conservatively, 115 mJ/m^2 for SiO_2, the work of adhesion, $W_{sn} = 2(\gamma_{SiO_2}\gamma_g)^{1/2}$, can be estimated to be 275 mJ/m^2 [26]. W_{sn} is thus reasonably close to the "threshold" work of an adhesion value of 330 mJ/m^2 obtained from the energetics analysis presented above.

Experiments have shown that a water layer might be present on a SiO_2 surface depending on the relative humidity. The thickness of the water layer is ~0.2 nm at 50% humidity and ~0.4 nm at 90% humidity [27]. It is possible that water could slightly wet a MWCNT. Water condensing into the small cavities between the MWCNT and the substrate surface by the capillary effect could then form a concave meniscus. The resulting Laplace pressure would provide an extra attractive force on the MWCNT in the region in contact with the meniscus. The meniscus curvature (r_c) can be estimated from the Kelvin equation, and is about 0.78 nm at 50% relative humidity [26]. The Laplace pressure (P_{LP}) can thus be estimated to be γ_{water}/r_c [28], which is about 100 MPa. (The force due to the surface tension of the meniscus circumference can be ignored since its radius is much larger compared to r_c. The surface energy γ_{water} of water is 72 mJ/m^2.) The binding energy between the surface and the MWCNT cylinder in the absence of capillary forces can be expressed as $W = AL\sqrt{R}/(12\sqrt{2}\,D^{3/2})$, where L is the length and R is the radius of the MWCNT, A is the Hamaker constant (a typical value of 10^{-19} J is used), and D is the typical Lennard-Jones distance of ~0.2 nm for the zero force condition. The resulting value of the binding energy is about one-sixth of the binding energy between the fully collapsed NT and the substrate. The van der Waals (vdW) interaction contribution in this uncollapsed NT/substrate setup is thus ignored.

An estimation of the contract pressure (P_{vdW}) between the flattened MWCNT and the substrate surface is also relevant. P_{vdW} can be estimated from considering two planar surfaces attracted to each other through vdW interactions ($P_{vdW} = A/6\pi D^3$). P_{vdW} is thus estimated to be about 700 MPa.

The energetics analysis shows that the vdW interaction between the flattened MWCNT and the substrate contributes significantly to the collapse of the MWCNT, and that the Laplace pressure P_{LP} is of the same order of magnitude as P_{vdW}. Thus, depending on the wettability of the MWCNT, the presence of water on the surface could have one of two diametrically opposing effects. If the MWCNT as well wetted by water, the Laplace pressure could significantly contribute to triggering and stability of collapse. In contrast, if the MWCNT was totally hydrophobic, due to the high dielectric constant of water (~80), the water layer would screen the energy of vdW interactions between the MWCNT and the substrate surface to approximately one-tenth of its value in air, precluding the deformation and collapse observed in our study. Thus, we may conclude that either MWCNTs are well wetted by water and their collapse was assisted by capillary forces or that a water layer was not present on the surface in our experiments and the collapse was mainly due to vdW interactions.

The observed 8-nm downward deflection of the collapsed section of MWCNT1 suspended above the trench in Fig. 1 was analyzed using a simple clamped-beam model [29]. The estimated value of the force necessary to cause the observed deflection was ~1 nN, comparable to the tapping force in our experiments, so the deflection could have been, in part, caused by the force applied by the tip. In any case, the observation clearly demonstrates the greater flexibility of the collapsed MWCNT section in comparison with the uncollapsed parts [Fig. 1(a)].

Another illustration of mechanical properties of collapsed NTs was provided by the observation of twists in the collapsed section of a different MWCNT (MWCNT2). As shown in Fig. 3(a), the 730-nm-long section of MWCNT2 extending out from the bottom left had a pillow shape and was collapsed all the way to the free end. The thickness (3.4 nm) of this section corresponds to a fully collapsed 5-cylinder MWCNT. Its inner and outer diameters in the undeformed cylindrical state were conservatively estimated to be equal to 5 and 8 nm, respectively. The estimated inner diameter of 5 nm for MWCNT2 is less than the critical diameter value for the collapse of a 5-cylinder MWCNT, which is between 8 and 16 nm according to Ref. [23]. Figures 3(b) and 3(c) show, respectively, the surface plots of the regions 1 and 2 marked by squares in Fig. 3(a). Figure 3(b) shows a twist that changed the orientation of the collapsed MWCNT2 with respect to the substrate surface as indicated by the gradual shift of the peak height in the surface height profiles of the pillow. Figure 3(c) shows the second twist that gradually changes the orientation. Remarkably, upon traveling from the substrate to the top of the deposit, the twisted section of MWCNT2 follows a straight line [Fig. 3(d)], in sharp contrast with the collapsed section in MWCNT1 that crosses the trench (Fig. 1). This strong anisotropy in flexibility of collapsed MWCNTs is quite intuitive and can be partly explained as a consequence of the differences of moments of inertia centered along different directions and mostly because of the high rigidity of the basal graphene sheet.

This work was supported by ONR and DARPA, the NSF ("New Tools and Methods for Nanotechnology"), and Zyvex, LLC. The authors appreciate Brian Faircloth for

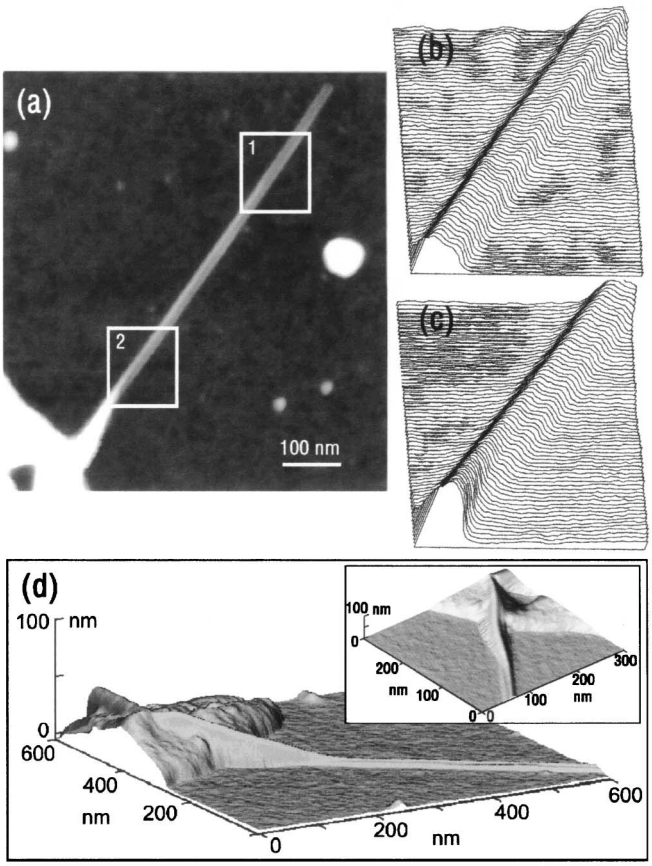

FIG. 3. (a) AFM image of a twisted and collapsed MWCNT (MWCNT2). (b) Surface plot of the square region 1 in (a) showing one twist. (c) Surface plot of the square region 2 in (a) showing another twist. (d) Three-dimensional side view of MWCNT2 where it extends from the deposit. The inset in (d) showing the three-dimensional top view of the twist in MWCNT2 where it extends from the deposit.

providing the trench patterned Si sample, Ed Kramer for useful comments, and Mark Dyer for help.

*Electronic address: tomek@andrew.cmu.edu
†Electronic address: r-ruoff@northwestern.edu

[1] B. I. Yakobson *et al.,* Comput. Mater. Sci. **8**, 341 (1997).
[2] J. P. Lu, J. Phys. Chem. Solids **58**, 1679 (1997).
[3] E. Hernandez *et al.,* Phys. Rev. Lett. **80**, 4502 (1998).
[4] E. W. Wong, P. E. Sheehan, and C. M. Lieber, Science **277**, 1971 (1997).
[5] A. Krishnan *et al.,* Phys. Rev. B **58**, 14 031 (1998).
[6] P. Poncharal *et al.,* Science **283**, 1513 (1999).
[7] J.-P. Salvetat *et al.,* Phys. Rev. Lett. **82**, 944 (1999).
[8] M.-F. Yu *et al.,* Science **287**, 637 (2000).
[9] O. Lourie, D. M. Cox, and H. D. Wagner, Phys. Rev. Lett. **81**, 1638 (1998).
[10] M. R. Falvo *et al.,* Nature (London) **389**, 582 (1997).
[11] R. S. Ruoff *et al.,* Nature (London) **364**, 514 (1993).
[12] J. Tersoff and R. S. Ruoff, Phys. Rev. Lett. **73**, 676 (1994).
[13] N. G. Chopra *et al.,* Nature (London) **377**, 135 (1995).
[14] V. Lordi and N. Yao, J. Chem. Phys. **109**, 2509 (1998).
[15] W. Shen *et al.,* Phys. Rev. Lett. **84**, 3634 (2000).
[16] M.-F. Yu, T. Kowalewski, and R. S. Ruoff, Phys. Rev. Lett. **85**, 1456 (2000).
[17] T. Hertel, R. E. Walkup, and P. Avouris, Phys. Rev. B **58**, 13 870 (1998).
[18] R. Martel *et al.,* Appl. Phys. Lett. **73**, 2447 (1998).
[19] C.-J. Park, Y.-H. Kim, and K. J. Chang, Phys. Rev. B **60**, 10 656 (1999).
[20] The sample was received from the Smalley group. The wafer substrate used in the experiments had a thin thermally grown SiO_2 layer on Si, and was patterned by electron beam lithography and plasma etching. The pattern on the surface consisted of 70-nm-wide, 17-nm-deep parallel trenches spaced 500 nm apart. A drop of the MWCNT 2-butanone suspension was placed on the substrate and dried at room temperature. The sample was examined by AFM (Multi-Mode Scanning Probe Microscope III-M, Digital Instruments) using standard silicon probes (TESP, Digital Instruments, nominal spring constant 50 N/m, resonance frequency ~300 kHz) operated in tapping mode in air. The AFM images were analyzed after a third-order baseline correction, eliminating the curvature due to the imperfection of the scanner. We acknowledge the use of the Cornell Nanofabrication Facility, where electron beam lithography and plasma etching were used to pattern trenches.
[21] J. S. Villarubia, J. Res. Natl. Inst. Stand. Technol. **102**, 425 (1997).
[22] The uncollapsed section was assumed to have the shape of an elliptic cylinder with a short ellipse axis $b = H_u/2$ and a long axis $a \geq b$, where H_u denotes the height of the uncollapsed section. The perimeter length of the uncollapsed section was calculated as $P_{ru} = 4aE(e)$, where $e = [1 - (b/a)^2]^{1/2}$, and $E(e)$ denotes the complete elliptic integral of the second kind. The results of consistency checks on perimeter lengths P_{ru} and P_{rc} for test shapes with the values of the length of the longer axis, $a \in \langle b, 1.5b \rangle$, are shown in Fig. 2(c) in the form of a plot of P_{rc}/P_{ru} vs a/b.
[23] L. X. Benedict *et al.,* Chem. Phys. Lett. **286**, 490 (1998).
[24] Malcolm E. Schrader and George I. Loeb, *Modern Approaches to Wettability (Theory and Applications)* (Plenum Press, New York, 1992), p. 70.
[25] P. Staszczuk, B. Janczuk, and E. Chibowski, Mater. Chem. Phys. **12**, 469 (1985); E. Papirer and H. Balard, in *The Surface Properties of Silicas,* edited by A. P. Legrand (Wiley, New York, 1998), pp. 315–364.
[26] J. N. Israelachvili, *Intermolecular & Surface Forces* (Academic Press, New York, 1997).
[27] F. Tiberg and A. M. Cazabat, Langmuir **10**, 2301 (1994).
[28] A. W. Adamson, *Physical Chemistry of Surfaces* (Wiley, New York, 1963).
[29] The force F necessary to produce the observed deflection $d_z = 8$ nm was estimated by considering the collapsed NT as a rectangular parallelpiped using the formula $F = 6EId_z/L^3$, where E is the Young's modulus, L is the length of the collapsed section spanning the trench, and I is the stress moment ($I = WD^3/12$). In the calculation, $E =$ 1000 GPa, $L = 70$ nm, $W = 9$ nm, and $D = 2.3$ nm.